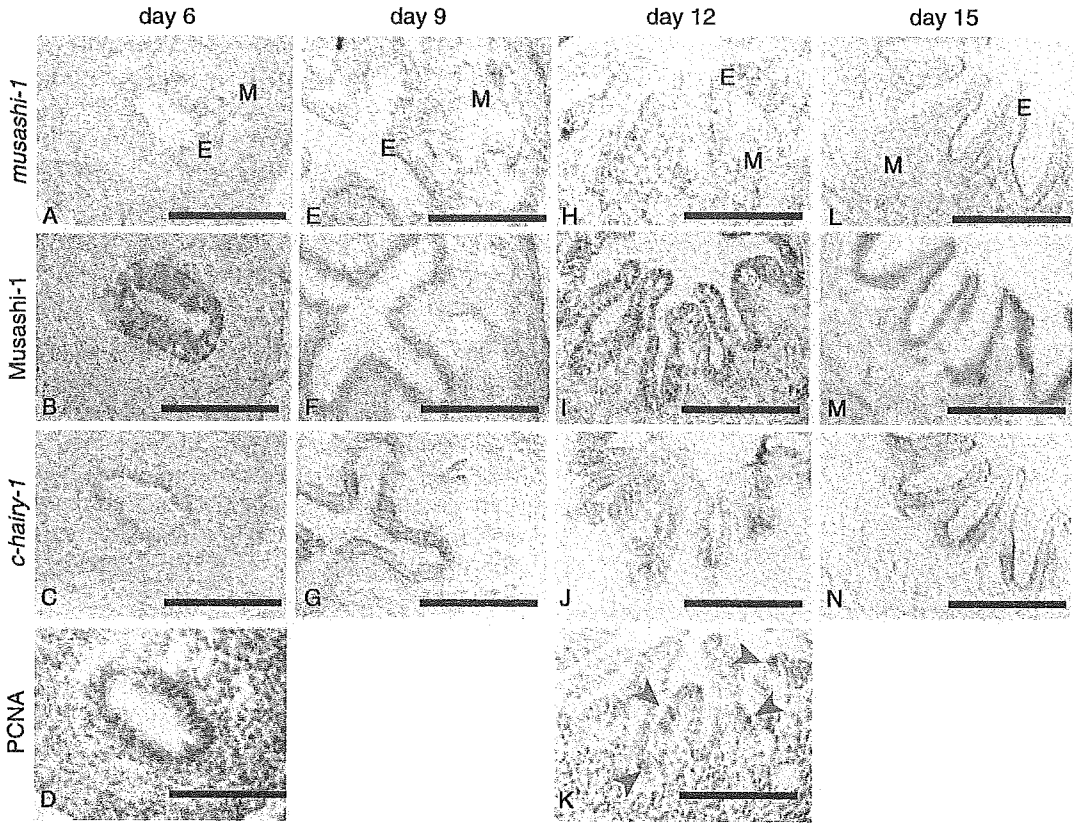

Fig. 1. Expression of mRNA (A,E,H,L) and protein (B,F,I,M) of *Msi-1* (A,B,E,F,H,I,L,M), *c-hairy-1* (C,G,J,N) and PCNA (D,K) in the developing chicken small intestine on day 6 (A–D), 9 (E–G), 12 (H–K) and 15 (L–N) of incubation. The *Msi-1* protein and mRNA expression patterns were identical. Red arrowheads indicate PCNA-positive cells (K). E, epithelium; M, mesenchyme. Bars, 100 μm.

Msi-1 mRNA and protein were found to be expressed in both the epithelium and the mesenchyme of the chick embryo from day 6 (Fig. 1A,B), and a similar expression pattern was observed until day 15 (Fig. 1E,F,H,I,L,M). In the mesenchyme, Msi-1 was observed to be expressed in the muscle layer (Fig. 1A.B). Expression of *c-hairy-1* was observed in both the epithelium and the mesenchyme on day 6 (Fig. 1C), whereas from day 9 to day 15, its expression was detectable only in the epithelium (Fig. 1G,J,N). PCNA-positive regions were detected in both the epithelium and the mesenchyme on day 6, but on day 12, positive staining of PCNA was observed in a few cells in the epithelium (Fig. 1D,K). Also in the epithelium, *Msi-1* and *c-hairy-1* showed coexpression and cells that were positive for these genes were also found to be positive for PCNA during the development of the chicken SI.

Expression of Msi-1 *in the adult chicken small intestine*

From day 15 of incubation, the chicken SI initiates the formation of crypts at the base of the villi and both the villi and crypts develop rapidly after hatching. The SI of the chicken at 14 days after hatching has therefore reached full maturity. Furthermore, *Msi-1* and *c-hairy-1* expression was observed to be restricted to the crypts (Fig. 2A–C) and these positive regions possessed high levels of proliferative activity (Fig. 2D). Moreover, when examined at a higher magnification, *Msi-1*-positive and *c-hairy-1*-positive regions were observed to be localized to almost identical regions of the crypts (Fig. 2E–G), and these areas were also found to be PCNA-positive (Fig. 2H). As it has already been shown in a number of studies that a stem cell zone exists in the crypts, this finding suggests that *Msi-1* is in fact a stem cell marker of the chicken SI epithelium. It is noteworthy also that in some epithelial cells of the adult chicken intestine, the Msi-1 protein is localized in the nucleus (Fig. 2B). Although the significance of this phenomenon is not yet known, a similar localization pattern has also been reported during the development of the inner ear (Sakaguchi *et al.* 2004).

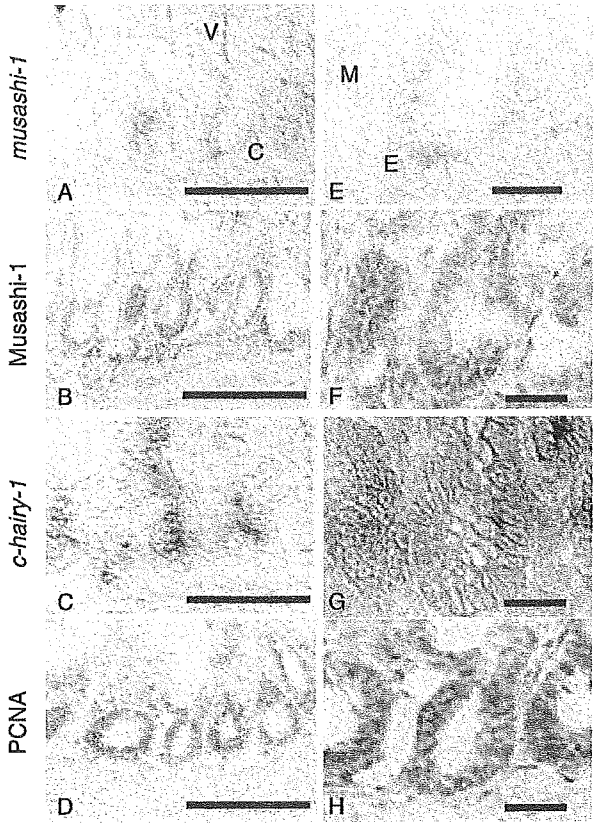

Fig. 2. Expression of mRNA (A,E) and protein (B,F) of *Msi-1* (A,B,E,F), *c-hairy-1* (C,G) and PCNA (D,H) in the chicken small intestine at 14 days after hatching. (E–H) Higher magnification of the crypt region. C, crypt; E, epithelium; M, mesenchyme; V, villus. Bars, 100 μm (A–D), 20 μm (E–H).

Expression of Msi-1 *during the development of the chicken proventriculus*

In chicken, the stomach is divided into two parts, the PV and the gizzard. In the PV, undifferentiated epithelium begins to invaginate into the underlying mesenchyme to form glands on day 6.5 of incubation. The glandular epithelium then gradually forms the compound glands from day 10 by repetitive branching (Romanoff 1960), whilst the non-invaginating luminal epithelium differentiates into villus-like structures from about day 14. On day 6 of incubation in our current experiments, both *Msi-1* and PCNA expression was observed in the epithelium and in the mesenchyme (Fig. 3A,B,D). On day 9, *Msi-1* was found to be expressed in both the luminal and glandular epithelia (Fig. 3E,F), but this became weaker in the luminal epithelium, although it remained at high levels in the glandular epithelium at later stages (Fig. 3H,I,L,M). *c-hairy-1* expression was detected in the epithelium on day 6 (Fig. 3C), but from days 9–12 its expression was restricted to the luminal epithelium (Fig. 3G,J,N). On day 12, PCNA-positive cells were detected in both the luminal and glandular epithelia (Fig. 3K). Cell proliferation levels were also found to be high in the region, which later forms secretory duct epithelium (Fig. 3K).

Expression of Msi-1 *in the adult chicken proventriculus*

After hatching, the epithelium of the chicken PV quickly matures. The luminal epithelium develops into fully grown villus-like structures and the glandular epithelium forms secreting ducts and many gland lobes. *Msi-1* was observed to be strongly expressed throughout the entire glandular epithelium and in the lower region containing the villus-like structures of the luminal epithelium (Fig. 4A,B). In contrast, *c-hairy-1* was found to be strongly expressed in the luminal epithelium and in the epithelium of the secretory ducts (Fig. 4C). PCNA-positive cells were evident in the secretory ducts, the lower parts of the villus-like luminal epithelium and throughout the glandular epithelium (Fig. 4D). Hence, it is evident that *Msi-1* gene expression and cell proliferation activity do not always coincide. These data therefore suggest that the association between *Msi-1* and *c-hairy-1* expression and cellular proliferation in the adult chicken PV is not equivalent to their relationship in the SI.

Expression of Msi-1 during the development of the mouse small intestine

The morphogenesis and differentiation of the epithelium in the mouse SI can be divided into four steps: (i) the epithelial cells proliferate rapidly and become stratified; (ii) numerous intraepithelial vacuoles are produced that fuse with the luminal surface on E13.5; (iii) mesenchymal cells invade the epithelium, and the stratified epithelium becomes a simple columnar structure on E15.5, and (iv) from E16.5, the epithelial cells differentiate into both intestinal absorptive cells and goblet cells. The crypts of Lieberkuhn first appear on E18.5 (Fukamachi 1978).

We examined the localization of Msi-1 and Ki67 proteins by immunohistochemistry and detected Msi-1 expression in the epithelium and mesenchyme on E13.5 (Fig. 5A). On E15.5, Msi-1 was found to localize in the epithelium at the base of the villi (Fig. 5B), but later be restricted to the pre-crypt regions (Fig. 5C,E,G,I). In P21 mice, crypt formation has almost reached completion and more than two Paneth cells can be observed in each crypt base. Msi-1-positive

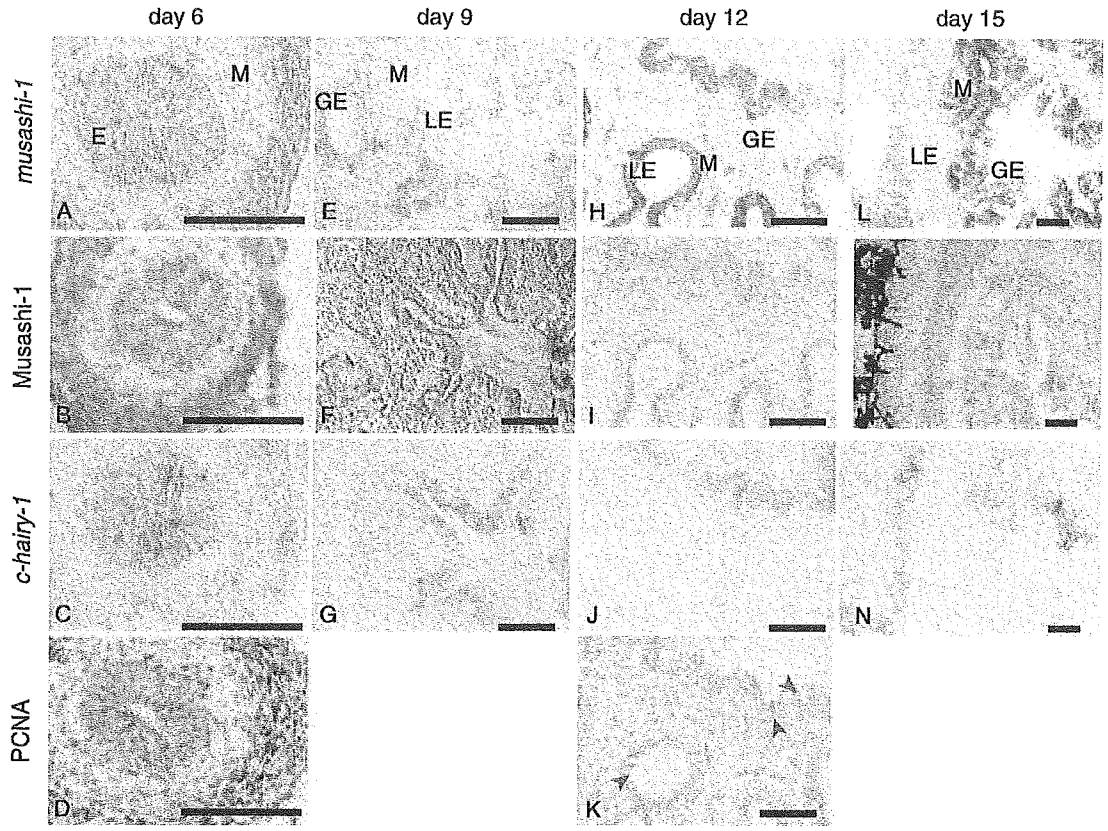

Fig. 3. Expression of mRNA (A,E,H,L) and protein (B,F,I,M) of *Msi-1* (A,B,E,F,H,I,L,M), *c-hairy-1* (C,G,J,N) and PCNA (D,K) of the developing chicken proventriculus on days 6 (A–D), 9 (E–G), 12 (H–K) and 15 (L–N) of incubation. E, epithelium; GE, glandular epithelium; LE, luminal epithelium; M, mesenchyme. Bars, 100 μm.

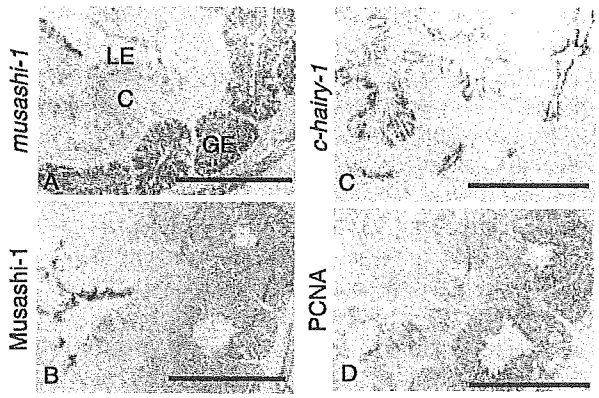

Fig. 4. Expression of mRNA (A) and protein (B) of *Msi-1* (A,B), *c-hairy-1* (C) and PCNA (D) in the chicken PV at 14 days after hatching. CT, connective tissue; GE, glandular epithelium; LE, luminal epithelium. Bars, 1 mm.

cells were observed to be localized just above the Paneth cells, and in the crypt base between them, at stage P21, and this expression pattern persisted until adulthood (Fig. 5K). In the epithelium, the zone of proliferative activity, assessed by Ki67 staining, very closely resembled the expression profile of Msi-1 (Fig. 5B,D,F,H,J,L). It was previously shown that both Msi-1-positive and Ki67-positive cells co-localize with *Hes1* expression at E13.5, E18.5 and at postnatal stages (Schroder & Gossler 2002).

Expression of Msi-1 during the development of the mouse stomach

In the mouse, the stomach is divided into the esophageal and the glandular regions. The epithelium of the former is pluristratified, in a similar manner to the esophagus, whereas that of the latter adopts a simple columnar structure and forms gastric glands (Fukamachi 1978). In the E11.5 mouse embryo, the stomach epithelium is pseudostratified and there is

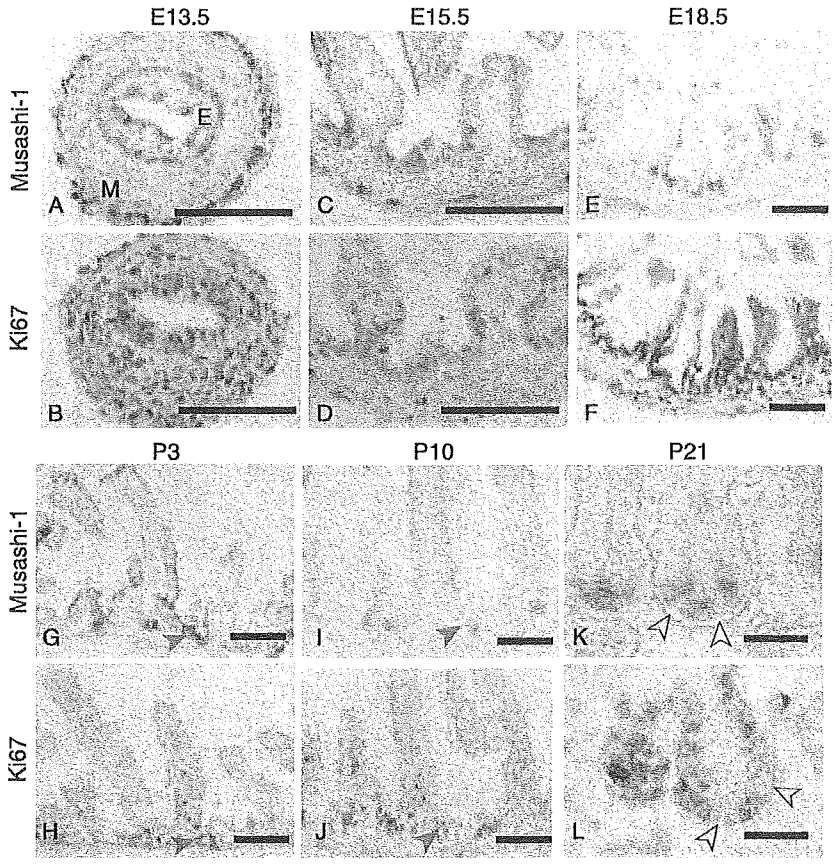

Fig. 5. Expression of Msi-1 (A,C,E,G,I,K) and Ki67 protein (B,D,F,H,J,L) in the developing mouse small intestine at stage E13.5 (A,B), E15.5 (C,D), E18.5 (E,F), P3 (G,H), P10 (I,J) and P21 (K,L). Red arrowheads indicate crypts and white arrowheads indicate Paneth cells. E, epithelium; M, mesenchyme. Bars, 100 μm (A–J), 20 μm (K,L).

little detectable difference between the presumptive esophageal and glandular regions. Morphological differences between the epithelia of the esophageal and glandular stomach regions can be observed at the E13.5 stage, at which point the epithelium of the esophageal region begins to stratify and becomes similar in appearance to the adult mouse by E18.5. In contrast, many intraepithelial vacuoles appear in the epithelium of the glandular region at stage E13.5, which are precursors of the pits or glands. Moreover, the formation of properly defined gastric glands can only first be observed in the newborn mouse. During the first 2 weeks of postnatal development these glands become larger and their cytodifferentiation is completed about 3 weeks after birth (Fukamachi 1978).

In our analyses of the esophageal region of the mouse stomach, at developmental stages E13.5 and E15.5, Msi-1 was found to be strongly expressed in the epithelium (Fig. 6A,C). Between E18.5 and adulthood, however, Msi-1 expression was barely detectable (Fig. 6E,G,I,K). At E13.5, Ki67-positive cells were scattered throughout the epithelium and mesenchyme (Fig. 6B), but after stage E15.5 the number of these positive cells was reduced and their localization in the mesenchyme was restricted to just below the epithelium (Fig. 6D,F,H,J). Furthermore, in the postnatal mouse Ki67-positive cells are found in the basal layer of the pluristratified epithelium (Fig. 6J,L,N).

In the glandular region of the E13.5 mouse stomach, Msi-1 was expressed in both the epithelium and the muscle layer (Fig. 7A). On E15.5, however, Msi-1 was not detectable in the epithelium (Fig. 7C), but its expression was reactivated in the epithelium by E18.5 (Fig. 7E). In P3 and P10 mice, Msi-1-positive cells were evident in the surface epithelium and in the lower halves of glandular epithelium (Figs 7G.I). Furthermore, in the adult mouse, Msi-1 was expressed in the neck and base regions of the glandular epithelium. In addition, the proliferative activity of the cells in the glandular region of the stomach during E13.5 could be widely observed in the whole tissues (Fig. 7B), but became gradually restricted to the glandular epithelium from E15.5 to P10 (Fig. 7D,F,H,J). In the adult mouse, the regions showing proliferative

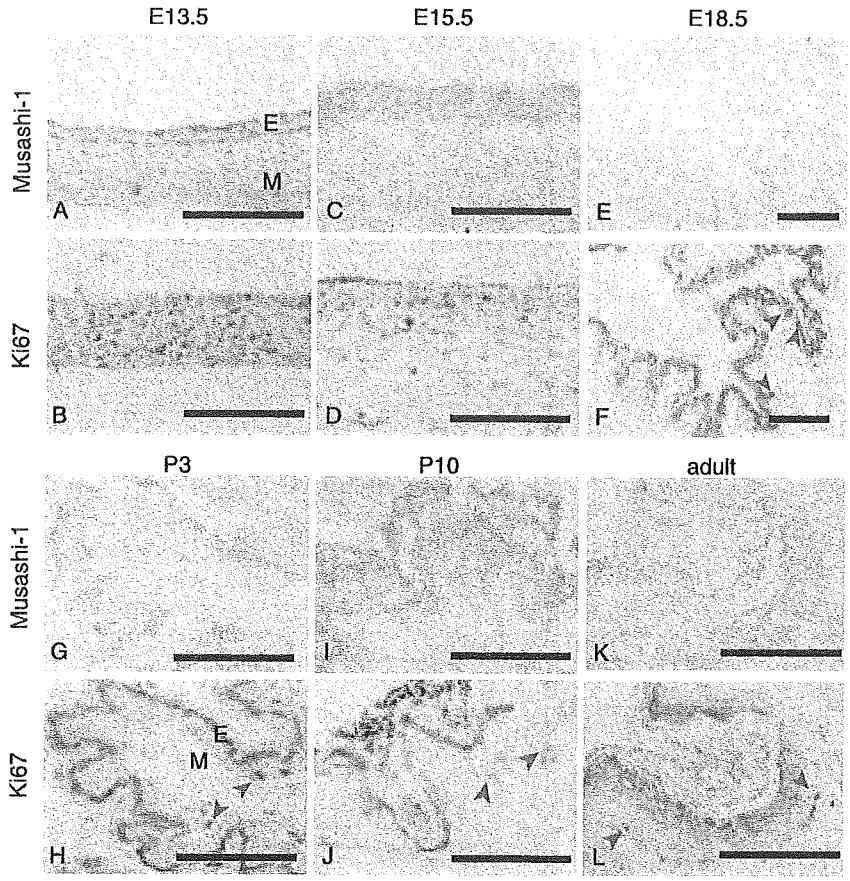

Fig. 6. Expression of Msi-1 (A,C,E,G,I,K) and Ki67 protein (B,D,F,H,J,L) in the esophageal region of the mouse stomach at stage E13.5 (A,B), E15.5 (C,D), E18.5 (E,F), P3 (G,H), P10 (I,J) and adult (K,L). Red arrowheads indicate PCNA-positive cells (F,H,J,L). Strong reactivity at the surface of the epithelium is due to the presence of mucus. Bars, 100 μm.

activity are located in the isthmus of the glands (Fig. 7L). Hence, the Msi-1- and Ki67-expressing regions were coincident in the glandular epithelium of the mouse from E18.5 to P10, but overlapped only partially in the adult mouse.

Discussion

Our present study demonstrates that *Msi-1* is expressed in both the epithelium and mesenchyme during the development of the chicken SI. Furthermore, we obtained almost identical results when we examined their expression profiles by either *in situ* hybridization or immunohistochemistry. In the mesenchyme, the expression of both of these factors is high in the smooth muscle layers in which the enteric ganglia are distributed. We could not however, distinguish smooth muscle cells and enteric ganglion cells in our current experiments.

In the epithelium of the developing chicken SI before day 15 of incubation, *Msi-1* is expressed ubiquitously. Cytodifferentiation of the SI epithelium begins from around day 7 to day 9 of incubation, when the expression of chicken intestinal fatty acid binding proteins and sucrase commences (Hiramatsu & Yasugi 2004). The ubiquitous expression of *Msi-1* may therefore be related to the onset of such SI-specific gene expression. The formation of villi starts at approximately day 15 of incubation and Msi-1 expression becomes gradually confined to the basal parts of the forming villi. This may be associated with the restriction of stem cell localization in the SI (Uni *et al.* 2000). Significantly, in both chicken and mouse, the expression of Msi-1 in the SI becomes gradually confined to the epithelium, suggesting that it is involved mainly in epithelial differentiation.

We further demonstrated in our current study that Msi-1 is also a marker of chicken SI stem cells. During the embryonic and post hatch development of the chicken SI, the epithelial regions that expressed both *Msi-1* and *c-hairy-1*, and that showed high proliferative activities, were strongly coincident. Similarly, in a previous study of the mouse SI epithelium, the expression of Msi-1 and the regions of cell proliferation activity co-localized, and the region of *Hes1* expression was also found to overlap with that of

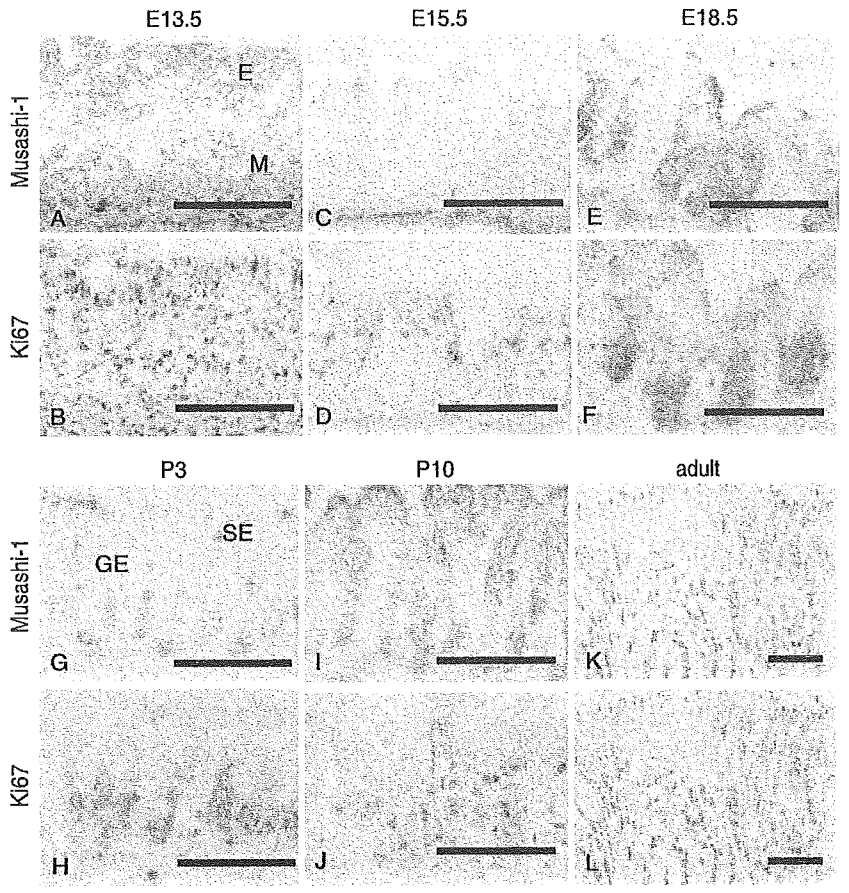

Fig. 7. Expression of Msi-1 (A,C,E,G,I,K) and Ki67 protein (B,D,F,H,J,E) in the glandular region of the mouse stomach at stage E13.5 (A,B), E15.5 (C,D), E18.5 (E,F), P3 (G,H), P10 (I,J) and adult (K,L). E, epithelium; GE, glandular epithelium; SE, surface epithelium. Bars, 100 μm.

Msi-1 (Kayahara *et al.* 2003). In the chick SI, *Msi-1* and *c-hairy-1* (*Hes1*) are expressed from the early stages of development and their expression patterns show dynamic changes. From these results we speculate that the expression of *Msi-1* in the chick SI is closely associated with cell proliferation, and that this effect may be transmitted by either Hes1 or c-hairy-1. It is therefore possible that the dynamic expression pattern of *Msi-1* reflects both the differentiation and localization of stem cell precursors of SI epithelial cells.

It has been previously demonstrated that Hes1 regulates the transcription of *Math1* and *ngn3*, and represses maturation of endocrine cells and Paneth cells (Jensen *et al.* 2000; Yang *et al.* 2001; Lee *et al.* 2002). Msi-1 has therefore a role in the maintenance of epithelial cells in an undifferentiated state and in the stimulation of morphogenesis. Presumably, these mechanisms of Msi-1 would ensure the properly timed differentiation of epithelial cells.

The chicken PV is unique among the glandular stomachs of vertebrates in that it has compound glands (Romanoff 1960). It was of great interest therefore to compare the expression patterns of Msi-1 and *c-hairy-1* in the PV, and also those of Msi-1 and *Hes1* in the mouse glandular stomach. Additionally, we wished to determine whether *Msi-1* is a candidate marker of gastric stem cells, as this would be an important aspect of the function of Msi-1 in the digestive organs. In the PV, the localization of *Msi-1* and *c-hairy-1*, and that of *Msi-1* and PCNA-positive cells, do not always coincide. Thus, the situation is different from that in the chicken SI and consequently it is difficult to hypothesize that *Msi-1* is in fact a marker gene of the stem cells in the stomach. This is also the case in the mouse glandular stomach, where the expression of *Msi-1* and *Hes1* does not co-localize (Kayahara *et al.* 2003). However, in the post-hatched chicken PV, the expression of Msi-1 in the lower half of the luminal epithelium, and also in the secretory duct epithelium, overlaps with both *c-hairy-1* and PCNA. This indicates that the cells in these regions are highly proliferative (Jin *et al.* 1996).

In our present study, the expression profile of *c-hairy-1* in the mouse stomach was wider than that of

Msi-1, which is consistent with the previously reported association of *Hes1* and *Msi-1* in the mouse stomach (Kayahara *et al.* 2003). This also indicates that the expression of *c-hairy-1* is not always regulated by Msi-1. In the esophageal stomach of the mouse, Msi-1 expression invariably diminished during the latter half of fetal development and there was no expression during the postnatal period. Since basal cells in the stratified epithelium are actively dividing, these results indicate that Msi-1 is not directly related to the proliferative activity of the epithelium. In the glandular stomach, the epithelium forms simple glands and the cell proliferation zone develops at the neck of the glands (Karam & Leblond 1993), which we also confirmed in the present study. The localization of Msi-1-positive cells overlapped partially with the area of proliferating cells, indicating that Msi-1 may also be expressed in stem cells. Cells expressing Msi-1 were found also in the deeper regions of the glands where differentiating cells, such as parietal cells and chief cells, reside.

In mammals, it has been shown that Hes1 controls the differentiation of endocrine cells in the stomach (Jensen *et al.* 2000). Moreover, there are several kinds of endocrine cells, that secrete hormones such as glucagons, secretin and somatostatin, present in the chicken PV (Rawdon 1984). Although at present it is not clear whether c-hairy-1 and Msi-1 are involved in the regulation of endocrine cell differentiation in the PV, it is highly possible that these gene products also play an important role in this structure.

Differentiation of the PV epithelium into the luminal and glandular epithelia is regulated by the transient expression of *Delta-1* and *Notch-1* in the undifferentiated epithelium at about day 6 of incubation (Matsuda *et al.* 2005). Cells expressing *Delta-1* induce *Notch-1* expression in the surrounding cells, and these cells become gland cells after they cease to express *Notch-1*. Although the expression patterns of *Msi-1* and *c-hairy-1* are almost identical on day 6 of incubation in the chick, *Msi-1* expression is soon after restricted to the gland epithelial cells and *c-hairy-1* expression is confined to the luminal epithelium. We can therefore speculate that there is an intimate relationship between Notch–Delta signaling and *Msi-1* and *c-hairy-1* expression.

Acknowledgements

We thank Dr O. Pourquié of the Developmental Biology Institute of Marseille for the gift of the plasmid containing *c-hairy-1*. We are also grateful to Dr H. Saiga and Dr K. Fukuda of Tokyo Metropolitan University for their valuable discussions and technical advice during the preparation of this manuscript. This work was supported in part by a Grant-in-Aid to S.Y. for Scientific Research on Priority Area (13044002) from the Ministry of Education, Culture, Sports, Science and Technology of Japan.

References

Akazawa, C., Sasai, Y., Nakanishi, S. & Kageyama, R. 1992. Molecular characterization of a rat negative regulator with a basic helix-loop-helix structure predominantly expressed in the developing nervous system. *J. Biol. Chem.* **267**, 21 879–21 885.

Booth, C. & Potten, C. S. 2000. Gut instincts: thoughts on intestinal epithelial stem cells. *J. Clin. Invest.* **105**, 1493–1499.

Coulombre, A. J. & Coulombre, J. L. 1958. Intestinal development. I. Morphogenesis of the villi and musculature. *J. Embryol. Exp. Morphol.* **6**, 403–411.

Fukamachi, H. 1978. The development of the gastro-intestinal tract of the mouse 1978. *J. Fac. Sci., Univ. Tokyo, Sec. IV.* **14**, 85–93.

Grey, R. D. 1972. Morphogenesis of intestinal villi. Scanning electron microscopy of the duodenal epithelium of the developing chick embryo. *J. Morphol.* **137**, 193–214.

Hinni, J. B. & Watterson, R. L. 1963. Modified development of the duodenum of chick embryos hypophysectomized by partial decapitation. *J. Morphol.* **113**, 381–425.

Hiramatsu, H. & Yasugi, S. 2004. Molecular analysis of the determination of developmental fate in the small intestinal epithelium in the chicken embryo. *Int. J. Dev. Biol.* **48**, 1141–1148.

Ishii, Y., Fukuda, K., Saiga, H., Matsushita, S. & Yasugi, S. 1997. Early specification of intestinal epithelium in the chicken embryo: a study on the localization and regulation of CdxA expression. *Dev. Growth Differ.* **39**, 643–653.

Ishizuya-Oka, A., Shimizu, K., Sakakibara, S., Okano, H. & Ueda, S. 2003. Thyroid hormone-upregulated expression of Musashi-1 is specific for progenitor cells of the adult epithelium during amphibian gastrointestinal remodeling. *J. Cell Sci.* **116**, 3157–3164.

Jarriault, S., Brou, C., Logeat, F., Schroeter, E. H., Kopan, R. & Israel, A. 1995. Signalling down stream of activated mammalian Notch. *Nature* **377**, 355–358.

Jensen, J., Pedersen, E. E., Galante, P. *et al.* 2000. Control of endodermal endocrine development by Hes-1. *Nat. Genet.* **24**, 36–44.

Jin, D.-Y., Ishii, Y. & Yasugi, S. 1996. Localization of DNA-synthesizing cells and cell proliferation pattern in developing proventricular (glandular stomach) epithelium of embryonic and hatched chickens. *Dev. Growth Differ.* **38**, 1–8.

Kaneko, Y., Sakakibara, S., Imai, T. *et al.* 2000. Musashi1: an evolutionally conserved marker for CNS progenitor cells including neural stem cells. *Dev. Neurosci.* **22**, 139–153.

Karam, S. M. & Leblond, C. P. 1993. Dynamics of epithelial cells in the corpus of the mouse stomach. Identification of proliferative cell types and pinpointing of the stem cell. *Anat Rec.* **236**, 259–279.

Kayahara, T., Sawada, M., Takaishi, H. *et al.* 2003. Candidate markers for stem and early progenitor cells, Musashi-1 and Hes1, are expressed in crypt base columnar cells of mouse small intestine. *FEBS Lett.* **535**, 131–135.

Lee, C. S., Perreault, N., Brestelli, J. E. & Kaestner, K. H. 2002. Neurogenin 3 is essential for proper specification of gastric enteroendocrine cells and the maintenance of gastric epithelial cell identity. *Genes Dev.* **16**, 1488–1497.

Matsuda, Y., Wakamatsu, Y., Kohyama, J., Okano, H., Fukuda, K. & Yasugi, S. 2005. Notch signaling functions as a binary switch for the determination of glandular and luminal fates of endodermal epithelium during chicken stomach development. *Development* **132**, 2783–2793.

Matsushita, S. 1983. Purification and partial characterization of chick intestinal sucrase. *Comp. Biochem. Physiol.* **76B**, 465–470.

Matsushita, S. 1985. Development of sucrase in the chick small intestine. *J. Exp. Zool.* **233**, 377–383.

Nakamura, M., Okano, H., Blendy, J. & Montell, C. 1994. MUSASHI, a neural RNA-binding protein required for Drosophila adult external sensory organ development. *Neuron* **13**, 67–81.

Ohtsuka, T., Ishibashi, M., Gradwohl, G., Nakanishi, S., Guillemot, F. & Kageyama, R. 1999. Hes1 and Hes5 as notch effectors in mammalian neuronal differentiation. *EMBO J.* **18**, 2196–2207.

Okano, H., Imai, T. & Okabe, M. 2002. Musashi: a transcriptional regulator of cell fate. *J. Cell Sci.* **115**, 1355–1359.

Potten, C. S., Booth, C., Tudor, G. L. *et al.* 2003. Identification of a putative intestinal stem cell and early lineage marker; musashi-1. *Differentiation* **71**, 28–41.

Rawdon, B. B. 1984. Gastrointestinal hormones in birds: Morphological, chemical and developmental aspects. *J. Exp. Zoo.* **232**, 659–670.

Romanoff, A. L. 1960. The Avian Embryo. Macmillan, New York.

Sakaguchi, H., Yaoi, T., Suzuki, T., Okano, H., Hisa, Y. & Fushiki, S. 2004. Spatiotemporal patterns of Musashi1 expression during inner ear development. *Neuroreport.* **15**, 997–1001.

Sakakibara, S., Imai, T., Aruga, J. *et al.* 1996. Mouse-Musashi-1, a neural RNA-binding protein highly enriched in the mammalian CNS stem cell. *Dev. Biol.* **176**, 230–242.

Sakakibara, S. I., Nakamura, Y., Yoshida, T. *et al.* 2002. RNA-binding protein Musashi family: roles for CNS stem cells and a subpopulation of ependymal cells revealed by targeted disruption and antisense ablation. *Proc. Natl Acad. Sci., USA* **99**, 15194–15199.

Sakakibara, S. & Okano, H. 1997. Expression of neural RNA-binding proteins in the postnatal CNS stem cell. *J. Neurosci.* **17**, 8300–8312.

Sasai, Y., Kageyama, R., Tagawa, Y., Shigemoto, R. & Nakanishi, S. 1992. Two mammalian helix-loop-helix factors structurally related to Drosophila hairy and Enhancer of split. *Genes Dev.* **6**, 2620–2634.

Schroder, N. & Gossler, A. 2002. Expression of Notch pathway components in fetal and adult mouse small intestine. *Gene Expression Patterns* **2**, 247–250.

Suzuki, K., Fukui, H., Kayahara, T. *et al.* 2005. Hes1-deficient mice show precocious differentiation of Paneth cells in the small intestine. *Biochem. Biophys. Res. Commun.* **328**, 348–352.

Takebayashi, K., Sasai, Y., Sakai, Y., Watanabe, T., Nakanishi, S. & Kageyama, R. 1994. Structure, chromosomal locus, and promoter analysis of the gene encoding the mouse helix-loop-helix factor HES-1. Negative autoregulation through the multiple N box elements. *J. Biol. Chem.* **269**, 5150–5156.

Uni, Z., Geyra, A., Ben-Hur, H. & Sklan, D. 2000. Small intestinal development in the young chick: crypt formation and enterocyte proliferation and migration. *Br. Poult Sci.* **41**, 544–551.

Yang, Q., Bermingham, N. A., Finegold, M. J. & Zoghbi, H. Y. 2001. Requirement of Math1 for secretory cell linage commitment in the mouse intestine. *Science* **249**, 2155–2158.

Available online at www.sciencedirect.com

SCIENCE DIRECT

Developmental Biology 286 (2005) 311 – 325

DEVELOPMENTAL BIOLOGY

www.elsevier.com/locate/ydbio

Visualization of spatiotemporal activation of Notch signaling: Live monitoring and significance in neural development

Jun Kohyama[a,b], Akinori Tokunaga[a,b], Yuko Fujita[a,b], Hiroyuki Miyoshi[c], Takeharu Nagai[d], Atsushi Miyawaki[d], Keiko Nakao[a,b], Yumi Matsuzaki[a,b], Hideyuki Okano[a,b,*]

[a]*Department of Physiology, Keio University School of Medicine, Tokyo 160-8582, Japan*
[b]*Core Research for Evolutional Science and Technology (CREST), Japan Science and Technology Corporation, Saitama 332-0012, Japan*
[c]*Subteam for Manipulation of Cell Fate, BioResource Center, RIKEN, Tsukuba Institute, Ibaraki 305-0074, Japan*
[d]*Laboratory for Cell Function and Dynamics, Advanced Technology Development Center, Brain Science Institute, RIKEN, 2-1 Hirosawa, Wako-city, Saitama 351-0198, Japan*

Received for publication 1 April 2005, revised 1 August 2005, accepted 3 August 2005

Abstract

Notch signaling plays various key roles in cell fate determination during CNS development in a context-dependent fashion. However, its precise physiological role and the localization of its target cells remain unclear. To address this issue, we developed a new reporter system for assessing the RBP-J-mediated activation of Notch signaling target genes in living cells and tissues using a fluorescent protein Venus. Our reporter system revealed that Notch signaling is selectively activated in neurosphere-initiating multipotent neural stem cells in vitro and in radial glia in the embryonic forebrain in vivo. Furthermore, the activation of Notch signaling occurs during gliogenesis and is required in the early stage of astroglial development. Consistent with these findings, the persistent activation of Notch signaling inhibits the differentiation of GFAP-positive astrocytes. Thus, the development of our RBP-J-dependent live reporter system, which is activated upon Notch activation, together with a stage-dependent gain-of-function analysis allowed us to gain further insight into the complexity of Notch signaling in mammalian CNS development.

Keywords: Notch; Hes1; RBP-J; Neural stem cell; Neural progenitors; Astrocyte; EGFP; Venus; Self-renewal; Gliogenesis

Introduction

Notch signaling plays a pivotal role in the organogenesis of many developing tissues in both vertebrates and invertebrates and controls cell fates through local cellular interactions; cells expressing Notch ligands communicate with neighboring cells that express Notch receptors (Artavanis-Tsakonas et al., 1999). Following the binding of the Notch receptor extracellular domain of Notch to its ligand, Delta/Serrate/lag-2 (DSL), the Notch receptor intracellular domain (NICD) (Weinmaster et al., 1991) is cleaved by presenilin/γ-secretase (Selkoe and Kopan, 2003). NICD is translocated into the nucleus and assembled into a complex with the DNA binding transcription factor, CSL (CBF1/RBP-J in mammals, suppressor of hairless in *Drosophila* and Lag-1 in *Caenorhabditis elegans*) (Kato et al., 1997), and the co-activator Lag3/Mastermind (Petcherski and Kimble, 2000). This complex then binds to specific *cis*-regulatory DNA sequences via CSL and induces the transcriptional activation of the target genes of the Notch signaling pathway, probably by recruiting p300 and other proteins into the transcriptional activation complex (Wu et al., 2000; Fryer et al., 2002; Wu et al., 2002; Maillard et al., 2003). In the absence of NICD, CSL can recruit repressor complexes to the *cis*-regulatory sequences of Notch target genes. The activation of Notch therefore acts as a switch that reverses the

* Corresponding author. Department of Physiology, Keio University School of Medicine, 35 Shinanomachi, Shinjuku-ku, Tokyo 160-8582, Japan.
E-mail address: hidokano@sc.itc.keio.ac.jp (H. Okano).

0012-1606/$ - see front matter © 2005 Elsevier Inc. All rights reserved.
doi:10.1016/j.ydbio.2005.08.003

transcriptional repression of its target genes (Barolo et al., 2002). In mammals, the basic helix–loop–helix (bHLH) genes *Hes1* and *Hes5* are considered to be primary targets of Notch because Notch activation induces the transcription of *Hes1* and *Hes5* (Kageyama and Nakanishi, 1997). Consistent with this hypothesis, the regulatory regions of these genes contain several RBP-J binding sites (Jarriault et al., 1995).

Several lines of evidence now indicate that Notch1-mediated signaling pathways play crucial roles in mammalian CNS development, including the maintenance of neural stem cell/progenitor states, the inhibition of neuronal cell commitment (Nye et al., 1994; Nakamura et al., 2000), and the promotion of astroglial fates (Gaiano and Fishell, 2002; Grandbarbe et al., 2003). However, the reported findings on the role of Notch signaling in neural development, especially in gliogenesis, remain controversial (Tanigaki et al., 2001; Hitoshi et al., 2002; Grandbarbe et al., 2003). The conflicting conclusions of previous reports can likely be partly attributed to the following facts: (i) functional redundancies in Notch-signal-related molecules and the early embryonic lethality of models carrying mutant forms (Ishibashi et al., 1995; de la Pompa et al., 1997; Ohtsuka et al., 1999) have prevented definitive conclusions in loss-of-function studies, and (ii) gain-of-function studies using an activated form of Notch sometimes have different outcomes, depending on the experimental conditions, because of the context-dependent actions of Notch-signaling.

As a first step towards addressing the complex role of Notch signaling during CNS development, we recently examined the in situ mapping of Notch1 activation using a specific antibody that recognizes the processed form of the intracellular domain of Notch1 after it has been cleaved by the activity of presenilin/γ-secretase (Tokunaga et al., 2004). However, this experimental system requires the cells to be fixed for the immunohistochemical analysis and cannot, therefore, be used to detect Notch1 activation in living tissue or to analyze the fate decision of cells in which Notch signaling had been activated in a prospective fashion.

To overcome these limitations, the initial goal of the present study was to generate a versatile live reporter system to detect the activation of Notch targets that are mediated by RBP-J. To establish such a reporter system, both a *cis*-regulatory element of the Notch target gene and a fluorescent protein are needed. For the *cis*-regulatory element of the Notch target gene, *Hes1* and *Hes5* are the strongest candidates because they are known targets of Notch signaling and they are expressed in the central nervous system. To exclude the possibility that the reporter gene transactivation was regulated by a signaling pathway other than RBP-J-mediated Notch activation, we utilized an RBP-J-dependent regulatory element in the endogenous target and we also employed a mutant promoter lacking the RBP-J recognition motif. We took advantage of the 195-bp promoter region of the *Hes1* gene (one of the endogenous target genes of Notch) that includes two RBP-J binding sites and several other elements known as E and N boxes (Sasai et al., 1992; Takebayashi et al., 1994; Jarriault et al., 1995). Since other *cis*-regulatory element may exist in this region, we also utilized a mutated form of the *Hes1* promoter (*Hes1*-pAmBm), in which two RBP-J binding sites are disrupted, to evaluate RBP-J-dependent *Hes1* promoter transactivation. We also developed a reporter system using an artificial promoter, TP-1, that includes 12 RBP-J binding sites and a minimum promoter (Kato et al., 1997). For live monitoring, a recently reported fluorescent protein Venus (and its destabilized form dVenus) (Nagai et al., 2002; Nagai et al., unpublished results) was utilized; this protein is an enhanced yellow fluorescent protein (EYFP) variant that exhibits fast and efficient maturation, a strong fluorescence intensity, and a tolerance to acidosis and Cl^- exposure (see the first paragraph of the Results section for further details).

In the present study, we clearly showed that our reporter system was sensitive enough to monitor the activated status of Notch signaling in living cells; the present reporter system could also be utilized in studies on the developing CNS as well as studies on the maintenance and differentiation of neural stem cells. Importantly, the new reporter system, in combination with a conventional stage-dependent gain-of-function study, enabled the dynamics of Notch signaling in cell-fate decisions during CNS development to be examined in detail.

Materials and methods

Gene construction of the reporter system

Venus and dVenus cDNA inserts (Nagai et al., 2002; Nagai et al., unpublished results) were substituted with pEGFP-1 and pEGFP-N1 (Clontech Laboratories) to generate pVenus-1/pdVenus-1 and pVenus/dVenus-N1, respectively. The 195-bp promoter region of *Hes1*p-luciferase (Jarriault et al., 1995) was subcloned into pVenus/dVenus-N1 and pVenus-1/pdVenus-1 to generate Hes1p-Venus/dVenus, respectively. We introduced mutations into both of the two RBP-J binding sites present within the 195-bp *Hes1* promoter region using site-directed mutagenesis to eliminate RBP-J binding activity, based on a strategy used in a previous study (Jarriault et al., 1995), and then constructed a *Hes1*pAmBm-dVenus/Venus variant. TP-1-Venus/dVenus and rBG-Venus/dVenus were generated by inserting the promoter region of TP-1 luciferase (Kato et al., 1997) and the minimal promoter region of TP-1 luciferase into pVenus/dVenus-1. To generate the mouse GFAP promoter-EGFP construct, a 2.5-kb fragment of the mouse GFAP promoter (Miura et al., 1990) was subcloned into pEGFP-1 (Clontech

Laboratories). To construct the lentivirus vectors, each *cis*-regulatory element and dVenus/Venus fragment was subcloned into a self-inactivating (SIN) vector construct (pCS-CG-PRE) (Miyoshi et al., 1999; Tahara-Hanaoka et al., 2002). In addition, the Notch1ΔE insert (Yamamoto et al., 2001b) was subcloned into the pEF-BOS expression vector (Mizushima and Nagata, 1990). The expression vector containing mouse full-length Notch1 was kindly provided by Dr. J. Nye. The expression vector containing a dominant-negative form of RBP-J has been described previously (Chung et al., 1994). The pMX-IRES-EGFP (IE) and NotchIC-pMXIE plasmids have also been reported (Hitoshi et al., 2002). Both EGFP and monomeric red fluorescent protein (mRFP) were subcloned into the mammalian expression vector pCXN2 (Niwa et al., 1991).

Cell culture

Telencephalons were dissected from ICR E14 mice, and after dissociation the cells were cultured via the neurosphere method as previously described (Reynolds et al., 1992; Kawaguchi et al., 2001; Shimazaki et al., 2001). For lentivirus transduction, a virus solution (with an MOI of 50) was added to the medium 3 h after the seeding of the cultures. For neurosphere formation, cells were cultured for 7–10 days. For γ-secretase inhibitor treatment of the primary neurospheres, a stock of L-685458 (Bachem) in DMSO was added to the medium at a concentration of 1 μM. Control treatments were performed using equivalent volumes of DMSO alone. The HEK293T cell line and NIH3T3 cell line were maintained in Dulbecco's modified Eagle medium (DMEM) supplemented with 10% fetal calf serum at 37°C in 5% CO_2.

Transient expression assay

The HEK293T cells were transfected with both 1 μg of the reporter constructs and 2 μg of the cDNA inserts in a pEF-BOS vector using Lipofectamine Plus reagent (Gibco-BRL). As for combined transfection of NotchΔE and RBP-J dn, we mixed each of these constructs at a ratio of 1:2 (2 μg of DNA in total). The cells were incubated for a further 24 h after transfection, followed by cell lysis and the determination of fluorescence intensities using a CytoFluor 4000 (PerSeptive Biosystems). The neurospheres were transfected with either pMXIE or NotchIC-pMXIE using a Nucleofector device (Amaxa), following the manufacturer's guidelines for the transfection of neural stem cells.

Cell preparation for flow cytometry and cell sorting

Flow cytometric analysis and cell sorting were performed using either a triple laser FACSVantage SE (Becton-Dickinson) or a MOFLO (DakoCytomation), as described previously (Kawaguchi et al., 2001). The cells in the viable gate were sorted into MHM medium and counted. A 50:49:1 cocktail of the resulting cell suspension, neurosphere-conditioned medium and B27 supplement (Gibco-BRL) was plated into each well of a 96-well plate at a density of 5 cells/μl (1000 cells/well), and the number of resulting neurospheres was counted approximately 14 days later. After the mechanical dissociation of each neurosphere into single cells, each pool of cells derived from a single neurosphere was cultured again for secondary neurosphere formation. For the differentiation assays, neurospheres that had been cultured for 10–14 days in vitro were plated onto poly-L-ornithine (PO)-coated coverslips and cultured for another 5–7 days in MHM medium.

In vivo electroporation

Pregnant ICR mice were purchased from Charles River, Japan; all animals were handled in accordance with the guidelines of Keio University. Both embryonic exo utero surgery and electroporation methods were performed as previously described (Muneoka et al., 1986; Saito and Nakatsuji, 2001). For the reporter analysis, DNA solutions (5 mg/ml in PBS containing FAST Green, Reporter: pCXN2-mRFP; 5:1) were injected into the lateral ventricle of E14 telencephalons. Electronic pulses of 25 V were charged eight times at 950-ms intervals using a square-pulse electroporator (CUY21EDIT; Nepa Gene Company). For the electroporation experiments in postnatal mice, P0 mice were anesthetized on ice and the injection and electroporation procedures were performed as described above except that an electric pulse setting of 50 V was used for the postnatal mice.

Lentivirus production

Lentiviral vectors, pseudotyped with the vesicular stomatitis virus G glycoprotein (VSV-G), were generated as previously described (Miyoshi et al., 1999).

Immunocytochemistry and immunohistochemistry

Immunocytochemical analysis of the cultured cells was performed as previously described (Kawaguchi et al., 2001). The primary antibodies used in this study were mouse monoclonal anti-MAP2 (mouse IgG, 1:500; Sigma), anti-β-III-tubulin (mouse IgG, 1:500; Sigma), anti-GFAP (rabbit IgG, 1:400; DAKO and mouse IgG, 1:400; Sigma), anti-O4 (mouse IgM, 1:2000; Chemicon), anti-GFP (rabbit IgG, 1:500; MBL), and rabbit anti-cleaved-Notch1 (actN1) (rabbit IgG, 1:500; Cell Signaling). For double staining, the cells were also incubated for 1 h with mixtures containing the secondary antibodies: Alexa Fluor 350-, 488-, 568, or 633-conjugated goat anti-mouse and anti-rabbit IgG (Molecular Probes). Samples were observed under a fluorescence microscope (Zeiss Axiophoto) equipped with the appropriate epifluorescence filters. Immuno-

histochemistry was performed as previously described (Kawaguchi et al., 2001; Tokunaga et al., 2004). Optical sections were viewed using a scanning laser confocal imaging system (Zeiss LSM510). To quantify the immunohistochemical data, we counted the cells using a Z-slice function.

Preparation of cell lysates and immunoblotting

Cells were centrifuged at 100 × *g* for 5 min, and the resulting cell pellets were lysed in 1× SDS–PAGE sample buffer. The subsequent immunoblotting procedure was performed as previously described (Tokunaga et al., 2004).

Results

Generation of a gene reporter system for activated Notch signaling

To visualize the activated status of Notch signaling, we developed a live reporter system based on the promoter region of a Notch signaling target and the Venus fluorescent protein (Fig. 1A). To detect the status of Notch signaling with a high time resolution, we incorporated a PEST sequence (Li et al., 1998), which is correlated with protein degradation, at the C terminus of Venus to create the fusion protein, dVenus (Nagai et al., unpublished). Our reporter

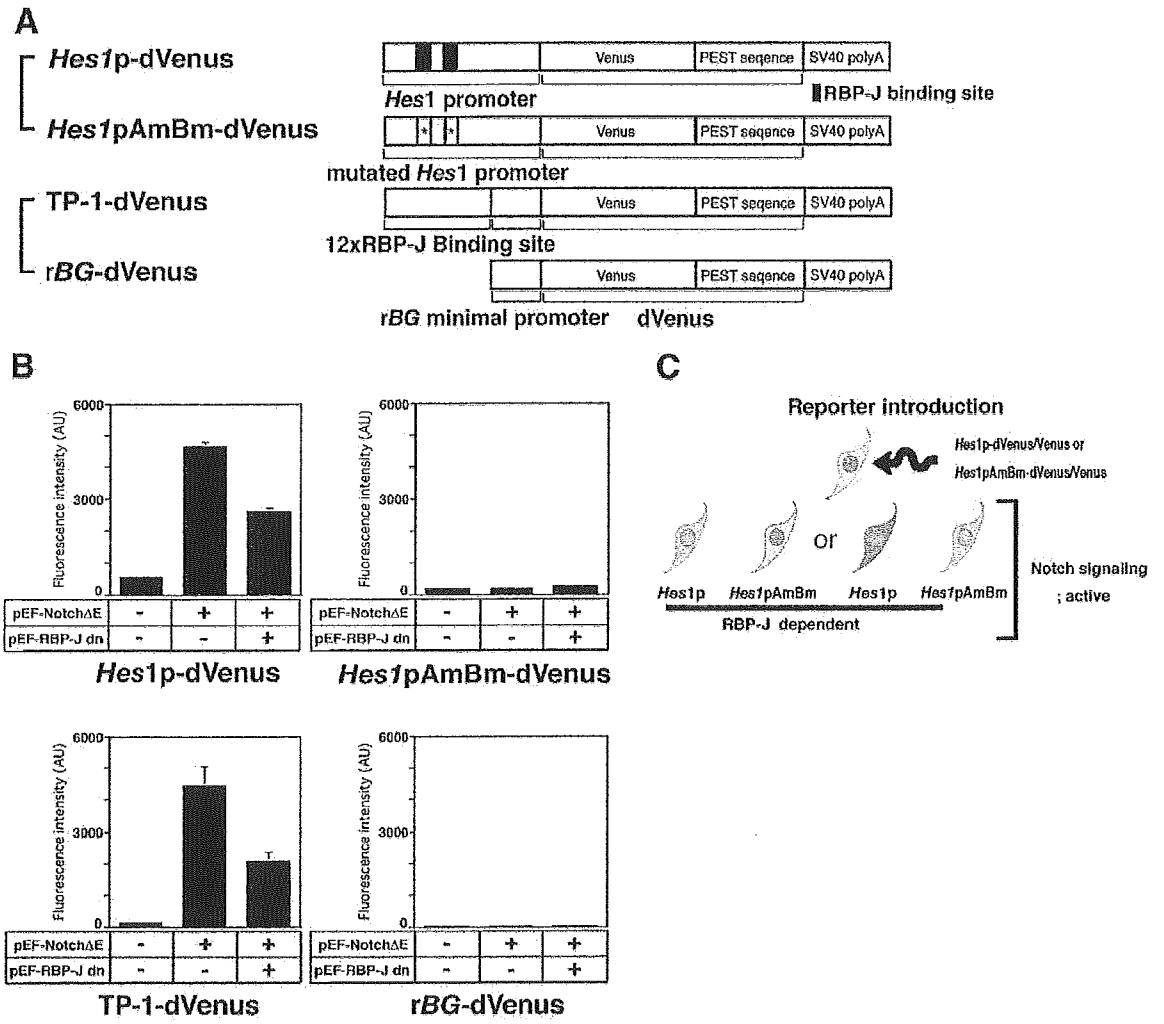

Fig. 1. Reporter systems for the detection of Notch activation. (A) Schematic representation of the reporter system (*represents disrupted RBP-J binding sites). (B) Notch signaling-dependent reporter activity according to fluorescent intensities assayed by transient transfection studies. (C) Basis for the detection of the RBP-J-dependent activation of Notch signaling in our analysis. Wild-type and mutated *Hes1* promoter-driven Venus fluorescence reactivity was compared. In the presence of Notch activation, the activity of the wild-type *Hes1* promoter should be stronger than that of the mutant promoter. Hence, the RBP-J-dependent activation of the Notch signaling target genes should be detectable. This was also the case for the functional analysis of Venus-positive cells. When the Venus-positive cell fractions driven by each promoter showed different neural cell characteristics, we regarded the differences between the Venus-positive cell fractions to reflect differences in the RBP-J-dependent Notch activity and function in those cell fractions. When no difference in the selectivity or reactivity of the two reporter-positive cell fractions was observed, we concluded that significant RBP-J-dependent activation was not involved in the context or cell-fate decision.

system consisted of two reporter sets based on both the 195-bp *Hes1* promoter region (Jarriault et al., 1995) (Hes1p-dVenus/Venus and *Hes1*pAmBm-dVenus/Venus) and an artificial promoter including 12 tandem RBP-J binding sequences plus a minimum promoter or a minimum promoter alone (TP-1-dVenus/Venus and rBG-dVenus/Venus) (Kato et al., 1997).

We first confirmed the reporter's sensitivity to the activation of Notch signaling in transient experiments using the combination of expression vectors shown in Fig. 1B. The intensity of the *Hes1*p-dVenus- and TP-1-dVenus-driven fluorescent signals was stronger (>8-fold) in the presence of Notch1ΔE than in the presence of PEF-BOS, whereas the reporter experiments using either *Hes1*-pAmBm-dVenus or rBG-dVenus constructs showed no response to Notch1ΔE. When both pEF-Notch1ΔE and the dominant-negative form of RBP-J (pEF-RBP-J dn) were co-expressed, the reporter fluorescence was less intense in cells expressing Hes1p-dVenus or TP-1 dVenus. Hence, our reporter system was strongly correlated with Notch signaling activity levels. Furthermore, *Hes1*p-dVenus and TP-1-Venus also showed Notch activity-dependent response in vitro; we could detect significant reporter activity in the presence of activated Notch1, not full-length Notch1 (Supplementary Fig. 1).

Next, we attempted to characterize the spatial and temporal profiles of RBP-J-dependent Notch activation to compare the differences between reporter sensitivities in the cells and tissue types analyzed in this study. We compared the Venus–fluorescence reactivity driven by the wild-type and mutated *Hes1* promoters, because the main purpose of this study was to examine the endogenous activation of Notch signaling during CNS development. Consistently, we could observe a relationship between active Notch1 immunoreactivity and reporter activity driven by *Hes1* promoter in vivo (Supplementary Fig. 2). Thus, the *cis*-regulatory element should be derived from the promoter region of endogenous Notch target genes.

The criteria for the detection of Notch activation in the experiment described below is described in Fig. 1C. Wild-type and mutated *Hes1* promoter-driven Venus fluorescence reactivity was compared. We need to compare this promoter set because the 195-bp *Hes1* promoter may contain target sequences for other signaling pathways. Thus, we can estimate the occurrence of RBP-J-dependent transactivation by observing the difference in reporter transactivation between wild-type and an RBP-J binding site-mutated promoter. In the presence of Notch activation, the activity of the wild-type *Hes1* promoter should be stronger than that of the mutant promoter. Hence, RBP-J-dependent activation of the Notch signaling target genes should be detectable (Fig. 1C). Regarding the functional assay, the Venus-positive cell fractions driven by the wild-type and mutant *Hes1* promoters exhibited different characteristics from those of neural cells; thus, the difference for each Venus-positive cell fraction reflects RBP-J-dependent Notch activity and function. We also examined the reporter activity of TP-1-dVenus/Venus and its control rBG-dVenus/Venus (Kato et al., 1997) with regard to their regulatory elements to confirm the occurrence of RBP-J-dependent Notch activation.

Enrichment of neurosphere-initiating cells based on Notch signaling activity

Previous studies have shown that Notch signaling activity is essential for the self-renewal of neural stem cells (Ishibashi et al., 1994; Ohtsuka et al., 1999; Nakamura et al., 2000; Hitoshi et al., 2002). Hence, we further investigated this relationship by monitoring embryonic neural cells using our reporter system. For this purpose, lentiviral vector constructs carrying each of our reporter gene inserts were generated, since lentiviral vectors are known to facilitate highly efficient and stable transduction into stem cells (Miyoshi et al., 1999). To directly determine the correlation between the reporter transactivation and the cell properties, we subjected embryonic brain cells that had been transduced with reporter lentivirus to fluorescence-activated cell sorting (FACS). We could observe the dVenus-derived reporter activity on embryonic cortical cells transduced by the lentiviral vector under physiological conditions (Supplementary Fig. 3A). To confirm the specificity of the response of reporter system, we treated reporter-carrying cells with a γ-secretase inhibitor, which was known to block Notch activation via suppression of the cleavage of the intracellular domain of Notch (Martys-Zage et al., 2000) (Supplementary Figs. 3B and C). We could see a reduction in the number of Venus-positive cell fraction in wild-type *Hes1* promoter Venus-transduced cells by FACS analysis, indicating that wild-type 195-bp *Hes1* promoter faithfully mimic Notch activity (Supplementary Figs. 3B and C, left panel, respectively). Therefore, our lentiviral reporter system was also effective for detecting the activation of Notch signaling. Regarding to the results of our experiments using mutant *Hes1* promoter, we could not detect any significant response to Notch activation in the *Hes1*AmBm reporter-transduced cells. Although there appeared to be a tendency towards increase in the activity of the *Hes1*AmBm reporter in response to a dose of γ-secretase inhibitor, we could not detect any statistically significant difference (Supplementary Figs. 3B and C, right panel, respectively). However, it is noteworthy that the activity of the *Hes1*pAmBm reporter activity was insensitive to the Notch activity. In this sense, we could not rule out the possibility that either non-RBP-J-mediated or non-Notch signaling are reported by our reporter constructs. Therefore, to unveil the circumstances of Notch activation, it is important to compare the response or distribution of wild-type and mutant *Hes1* promoter transactivation.

Cortical cells, derived from E14 embryos, were cultured to produce neurospheres using a selective culture method in which the neural precursors selectively survived and

proliferated in response to EGF and FGF-2 (Reynolds et al., 1992). We then introduced pSIN-*Hes1*p-dVenus into these primary neurospheres, which were subsequently transferred to pre-coated cover slips and cultured in the presence of growth factors. In combination with an immunocytochemical analysis, selective *Hes1*p-dVenus-derived fluorescence was observed in Nestin-positive neural progenitors (Fig. 2A, upper panel) but rarely detected in β-III-tubulin-positive neurons (Fig. 2A, lower panel). Next, to further characterize the correlation between Notch signaling activation and stem cell maintenance, we performed a neurosphere assay and determined the number of neurosphere-initiating cells using a method described in our previous report that utilized the *Nestin*-EGFP reporter gene (Kawaguchi et al., 2001). Each reporter construct was introduced into dissociated E14 cortical cells, and the fluorescent cells were sorted by flow cytometry after 24 h. The sorted cells were then cultured at a cell density of 5 cells/μl, which is below the cell density at which virtually all neurospheres are clonal cells (Hulspas et al., 1997). At 10–14 days, the sphere numbers were counted per 1000 reporter-gene-expressing cells and were found to be 28.9 ± 6.8 and 8.5 ± 1.50 in *Hes1*p-dVenus-expressing and *Hes1*pAmBm-dVenus-expressing cells, respectively ($P < 0.05$). In addition, the efficacy of neurosphere formation from *Hes1*pAmBm-dVenus-expressing cells did not differ from that of control EF-dVenus-expressing cells ($P > 0.05$). The number of sphere-initiating cells was therefore significantly higher among the *Hes1*p-dVenus-expressing population, compared to EF-

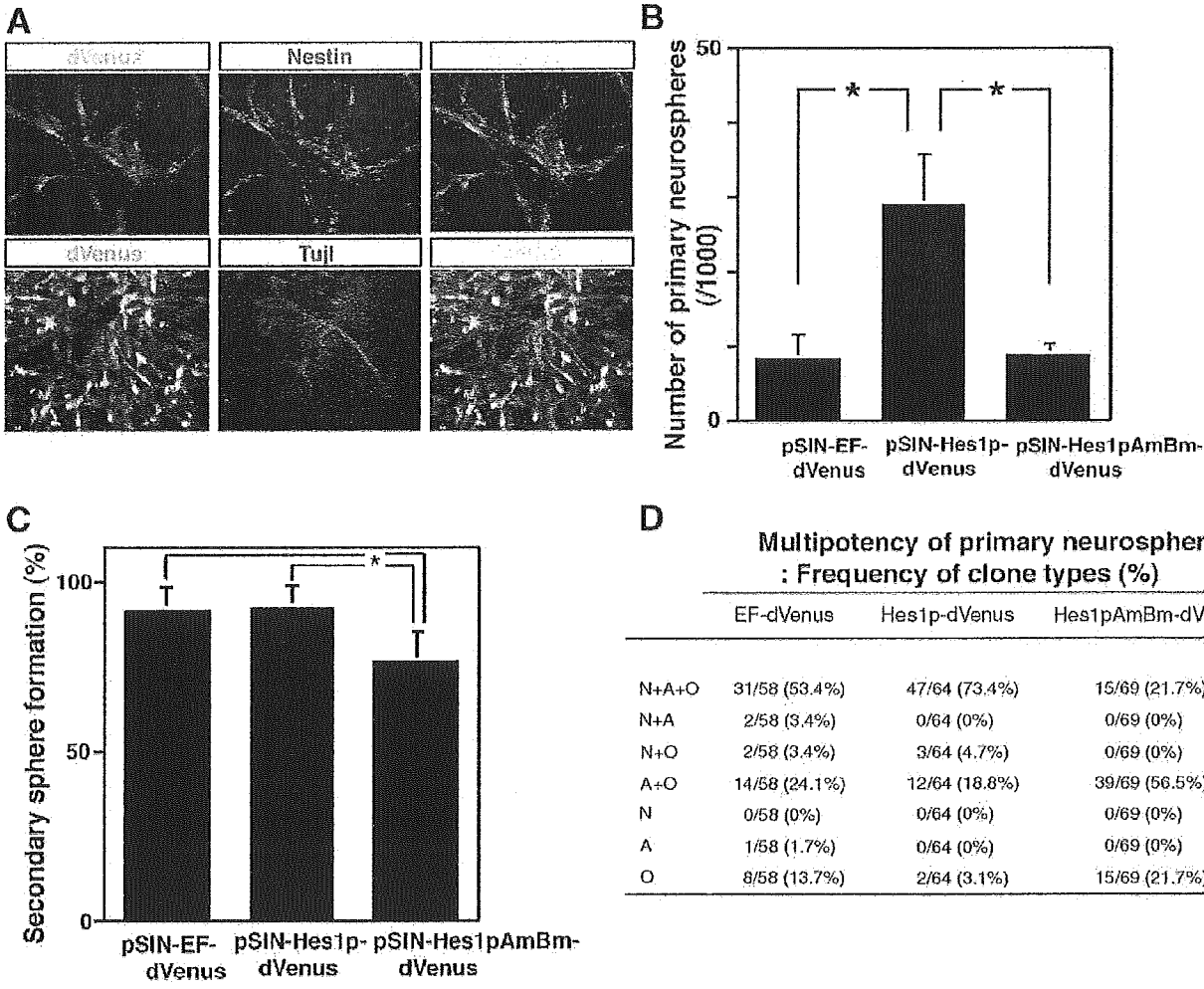

D

Multipotency of primary neurospheres : Frequency of clone types (%)

	EF-dVenus	Hes1p-dVenus	Hes1pAmBm-dVenus
N+A+O	31/58 (53.4%)	47/64 (73.4%)	15/69 (21.7%)
N+A	2/58 (3.4%)	0/64 (0%)	0/69 (0%)
N+O	2/58 (3.4%)	3/64 (4.7%)	0/69 (0%)
A+O	14/58 (24.1%)	12/64 (18.8%)	39/69 (56.5%)
N	0/58 (0%)	0/64 (0%)	0/69 (0%)
A	1/58 (1.7%)	0/64 (0%)	0/69 (0%)
O	8/58 (13.7%)	2/64 (3.1%)	15/69 (21.7%)

Fig. 2. Role of neuronal progenitors maintenance during mouse embryonic CNS development. (A) *Hes1*p-driven signals were selectively observed in mouse neural progenitors. Most of the Venus-positive cells were Nestin-positive neural progenitors (upper panel), whereas Venus-fluorescence was not observed in β-III-tubulin-positive neurons (lower panel). (B) Comparison of the efficiency of the neurosphere-formation potency of reporter-responsive cells. Neurosphere-initiating efficiency was significantly increased in *Hes1*p-dVenus-positive cells, compared to that in either *Hes1*pAmBm- or EF-dVenus-positive cells ($n = 4$ in EF, $n = 7$ in *Hes1*p and *Hes1*pAmBm) (*$P < 0.05$). (C) Secondary neurosphere formation efficacy. A reduction in secondary sphere formation was observed in primary neurospheres derived from *Hes1*pAmBm-dVenus-expressing cells (*$P < 0.05$). (D) Multilineage potentials were confirmed by immunocytochemical analysis of the neurons (anti- β-III-tubulin), astrocytes (anti-GFAP), and oligodendrocytes (anti-O4). The number of clones consisting of neurons (N), astrocytes (A), or oligodendrocytes (O) is shown as a percentage of the total number of clones.

dVenus- and *Hes1*pAmBm-dVenus-expressing cells. To examine the capacity of the sorted Venus-positive cells for self-renewal, the secondary neurosphere-forming efficiency of each primary neurosphere was compared to estimate the frequency of self-renewing cell division arising from the original neurosphere-producing cell (Nakamura et al., 2000; Kawaguchi et al., 2001) (Fig. 2C). We subsequently observed a reduction in the number of secondary neurospheres derived from *Hes1*pAmBm-dVenus-expressing cells compared to those from *Hes1*p-dVenus-expressing cells ($P < 0.05$).

We next examined whether the neurospheres generated from the reporter-responsive cells showed any disruption in their multipotent properties, since a certain percentage of neurospheres derived from committed progenitor cells was previously shown to differentiate only into specific lineages (Reynolds and Weiss, 1996). Primary neurospheres, generated after FACS-sorting, were clonally transferred onto pre-coated cover slips to obtain one neurosphere culture per well. These cells were then cultured without growth factors and processed for triple-labeled indirect immunocytochemistry after 5 days to detect the three major cell types, neurons, astrocytes, and oligodendrocytes, using anti-β-III-tubulin, anti-GFAP, and anti-O4 antibodies, respectively (Fig. 2D). More than 70% of the *Hes1*p-dVenus-derived neurospheres were multipotent and differentiated into clones containing neurons, astrocytes, and oligodendrocytes (NAO). However, about 20% of the neurospheres were bipotent, generating either neurons and oligodendrocytes (NO) or astrocytes and oligodendrocytes (AO). Furthermore, committed progenitors, which are capable of generating only restricted lineages, were rare in the neurospheres derived from *Hes1*p-Venus-positive cells (3.1%), but the differentiation capacity of the neurospheres derived from *Hes1*pAmBm-dVenus-positive cells showed a reduction in tripotent neurosphere formation and an increase in bipotent or monopotent neurosphere formation. The above results suggest that Notch signaling activity is positively correlated with both self-renewal and the multipotency of neural progenitors in an RBP-J-dependent manner, as shown by our Notch-dependent reporter system (Fig. 1C).

RBP-J-dependent Notch activation is observed in radial glia

We examined the in vivo distribution of reporter activity using an electroporation co-transfection method in the cortical ventricular zone (VZ) of E14 mice (Fig. 3A). The efficiency of co-transfection was confirmed using EGFP and monomeric red fluorescent protein (mRFP) constructs, driven by a pCXN2 promoter (>95%) (data not shown). Therefore, we examined the cellular distribution of positive reporter activity by analyzing the localization of mRFP-positive cells at 48 h post-transfection, when most of the transfected cells were located in the VZ intermediate zone (IZ) region. Very few positive cells were observed using the *Hes1*p-dVenus reporter gene. Thus, to substantially increase the number of fluorescence-positive cells, a Venus reporter gene, instead of dVenus, was used in the series of experiments shown in Fig. 3. Venus-derived signals, from the wild-type *Hes1* promoter, were mostly observed in the VZ regions and were morphologically characterized by the extension of radial fibers from the ventricular to the pial surface (Figs. 3B and F). These *Hes1*p-Venus-positive cells located in the VZ were also positive for Nestin (Supplementary Fig. 4A).

On the other hand, *Hes1*pAmBm reporter activity was also observed in the VZ, SVZ, or IZ. Most of these *Hes1*pAmBm-Venus-positive cells were located in the SVZ-IZ (Figs. 3C and F; Supplementary Figs. 4C and D). However, these cells did not possess apparent radial fibers. In the same series of experiments, another reporter set, utilizing TP-1, was introduced by electroporation (Figs. 3D and E). The reporter activity of TP-1 was also observed in cells exhibiting radial fibers (Fig. 3D), which were also positive for Nestin (Supplementary Fig. 4E); these results are consistent with those obtained using *Hes1p*-Venus (Fig. 3B). On the other hand, a reporter carrying only the rat β-globin minimal promoter (rBG-Venus) did not exhibit fluorescence (Fig. 3E). Taken together, it is likely that the wild-type *Hes1*p and TP-1 reporters are activated in the radial glia, which could be relevant to the results of our recent report showing the selective localization of active Notch1 immunostaining in the radial glia in this context (Tokunaga et al., 2004).

Notch signaling functions in astroglial commitment, but not in astroglial maturation

In view of our previous results showing a negative correlation between immunoreactivity to GFAP and the activated form of Notch1 (Tokunaga et al., 2004), we hypothesized that Notch signaling may be down-regulated during the terminal differentiation of astroglial cells expressing GFAP. However, the exact role of Notch signaling in astroglial development remains to be elucidated. To address the role of Notch signaling in astroglial development during the early postnatal stage, transgenes expressing the intracellular domain of Notch1 (NotchIC)-IRES-GFP (NotchIC-pMXIE) or EGFP (pMXIE) were introduced by electroporation into the VZ of P0 mice brains and their effects on the generation of astroglial cell lineages were analyzed at P8. We examined the expression of the astroglial marker GFAP in the EGFP-expressing cells in the periventricular area (Fig. 4). An experiment using control EGFP vector (pMXIE) revealed that some of the EGFP-positive cells were GFAP-positive astrocytes (Figs. 4A–C). In contrast, fewer NotchIC-IRES-EGFP-expressing cells were found to be GFAP-positive astrocytes (Figs. 4D–F). These results indicate that the ectopic expression of activated Notch1 resulted in a decrease in the number of GFAP-positive astrocytes (Fig. 4G) and that the persistent

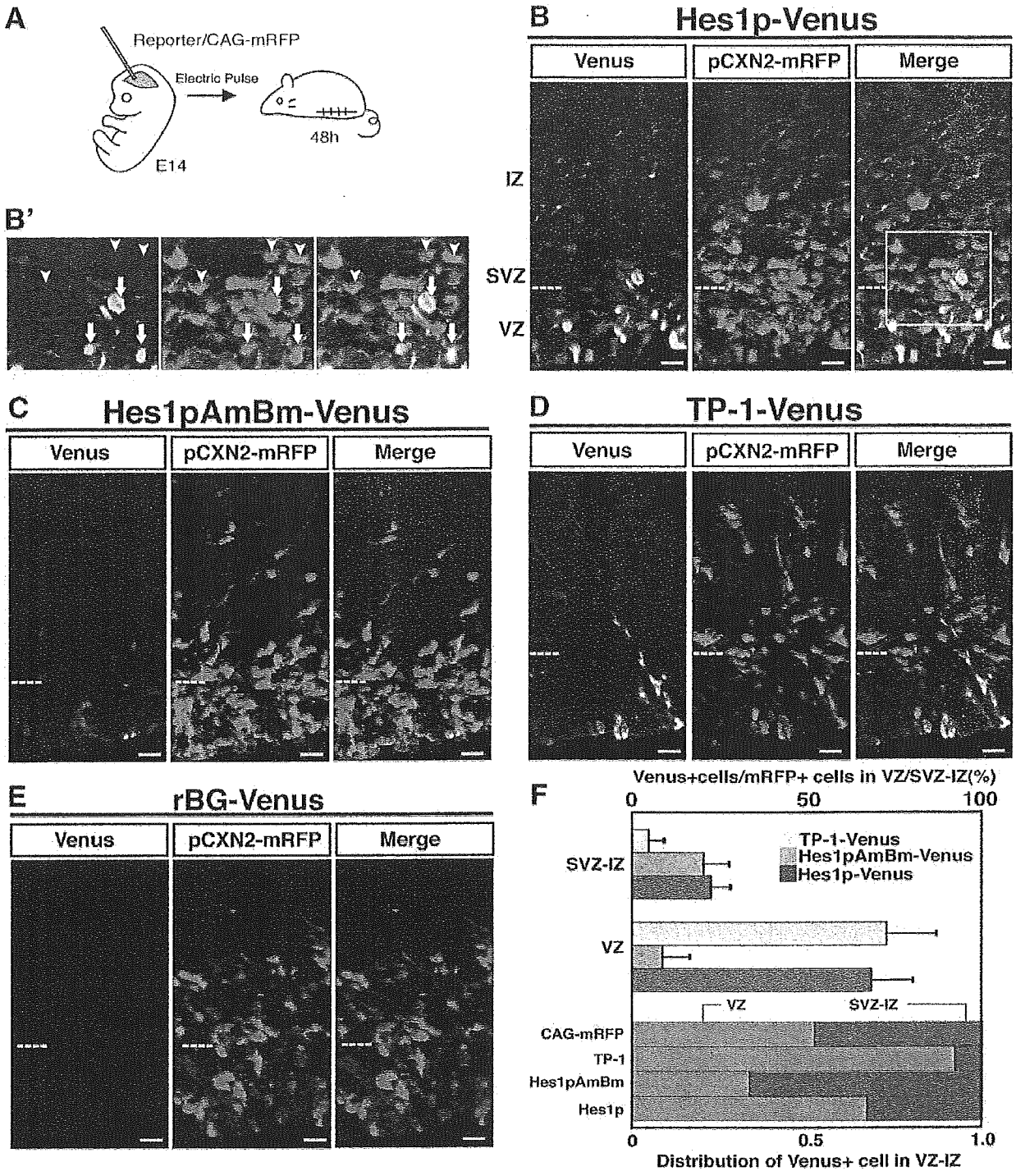

Fig. 3. Distribution of reporter activity in the developing cerebral cortex. (A) Schematic representation of the adopted in vivo electroporation procedure. (B) The distribution of *Hes1*p-Venus was mostly confined to cells in the VZ region, characterized morphologically by the presence of radial fibers. Some Venus-positive cells in the SVZ-IZ exhibited a multipolar morphology. (B′) Shows a higher magnification of the boxed region of panel B. (C) Venus fluorescence, driven by *Hes1*pAmBm, was also observed in the VZ and SVZ-IZ. (D) TP-1 Venus-driven signals were observed selectively in cells of the VZ, characterized by the presence of radial fibers. Cells in the SVZ-IZ only exhibited mRFP-signals. (E) rBG-Venus-driven signals were not observed. Scale bars: 10 μm. (F) Quantification of the distribution of cells exhibiting the activity of each reporter construct in the VZ and SVZ-IZ. We performed three independent experiments. VZ: ventricular zone; SVZ: subventricular zone; IZ; intermediate zone.

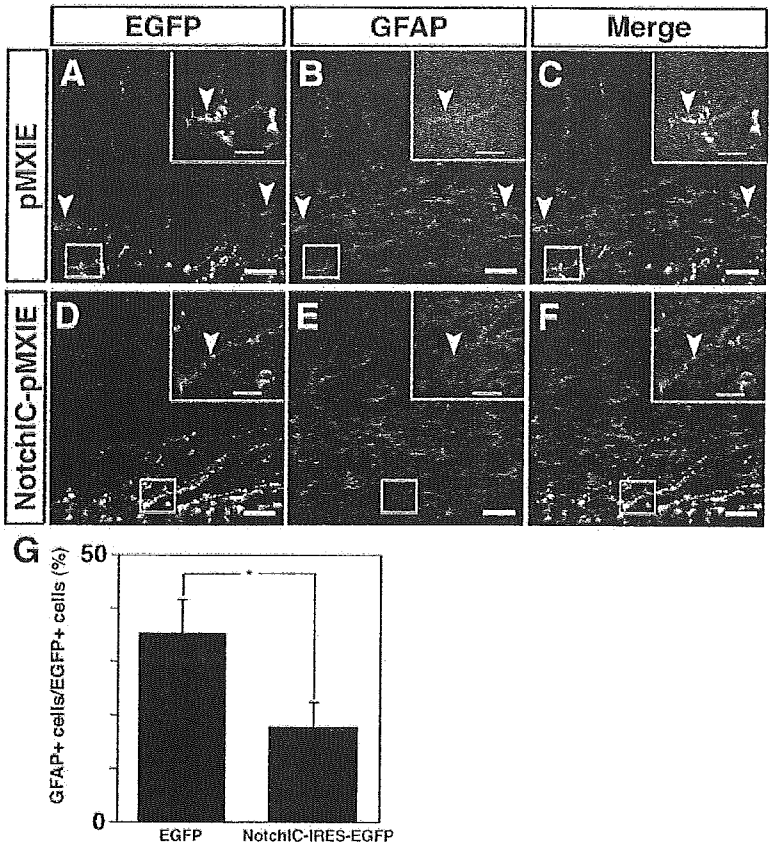

Fig. 4. Ectopic expression of the cleaved form of Notch1 in postnatal brain. The effect of Notch activation on astroglial differentiation was examined by introducing the intracellular domain of Notch1 (NotchIC)-IRES-EGFP- or control EGFP-expressing vectors in the P0 brain, and analyzing astroglial differentiation was analyzed in the P8 brain. Cells located around the VZ were examined for the expression of GFAP. (A–C) Characterization of control EGFP-vector-carrying cells. The insets represent a higher magnification of the boxed regions in each corresponding figure. (D–F) Characterization of NotchIC-IRES-EGFP-construct-expressing cells. The insets represent a higher magnification of the boxed region in each corresponding figure. (G) Quantitative analysis of the signals in these experiments ($^*P < 0.05$, $n = 3$, respectively). Scale bars: A–F: 50 μm; inset box: 20 μm.

activation of Notch signaling reduced the number of GFAP-positive astrocytes at an early postnatal stage.

However, whether this observed phenotype occurs at the commitment or maturation of astroglial cells remains uncertain. To address this issue, we investigated the role of Notch signaling activation on astroglial development using primary neurospheres derived from E14 cortex under differentiation conditions, in which the neurospheres were cultured without growth factors on pre-coated cover slips (Fig. 5A). First, we examined the expression level of the cleaved form of Notch1 and GFAP during the differentiation of neurospheres using immunoblot studies (Fig. 5B). We found that the expression of the cleaved form of Notch1 was down-regulated, while GFAP expression was up-regulated, during the differentiation of the neurospheres. Thus, the amount of the cleaved form of Notch1 was negatively correlated with the GFAP expression level during the differentiation phase, indicating that Notch signaling may be selectively activated during astroglial commitment rather than at astroglial maturation. The significance of early stage Notch activation in astroglia generation was further confirmed by γ-secretase inhibitor treatment under differentiation conditions (Fig. 5C). We treated primary neurospheres with the γ-secretase inhibitor from the beginning of the differentiation phase. The temporal expression patterns of the markers that were employed were then examined using immunocytochemistry: MAP2 for neurons, and GFAP for astrocytes. Neurospheres treated with DMSO as a negative control spontaneously differentiated into these two lineages (MAP2 positive: 33.1 ± 9.2%; GFAP positive: 41.5 ± 13.4%) (Fig. 5C, upper left and lower left panel). On the other hand, neurospheres treated with γ-secretase inhibitor induced an increase in MAP2-expressing cells (52.0 ± 18.0%) and a reduction in GFAP-expressing cells (7.0 ± 4.5%) (Fig. 5C, upper right and lower right panel). When γ-secretase inhibitor was added during the late phase of differentiation, i.e., 3–5 days after culturing the primary neurospheres on coated coverslips in MHM without growth factors, the number of resulting GFAP-positive astrocytes was not altered (data not shown). Thus, Notch activation is required for astrogliogenesis in the early phase of the differentiation of neurosphere-derived cells.

We subsequently examined whether the persistent activation of Notch signaling could suppress the generation

of GFAP-positive astrocytes in a neurosphere differentiation assay. The intracellular domain of Notch1 (NotchIC) was introduced into primary neurospheres followed by plating on pre-coated coverslips in medium without growth factors (Figs. 5A and D). We analyzed the cell type of NotchIC or control vector-carrying cells after 4 days. A reduction in the number of GFAP-positive astrocytes generated from NotchIC-expressing cells was observed (Fig. 5D), possibly corresponding with the Notch1-persistent activation results observed during the early neonatal stage in vivo (Figs. 4D–

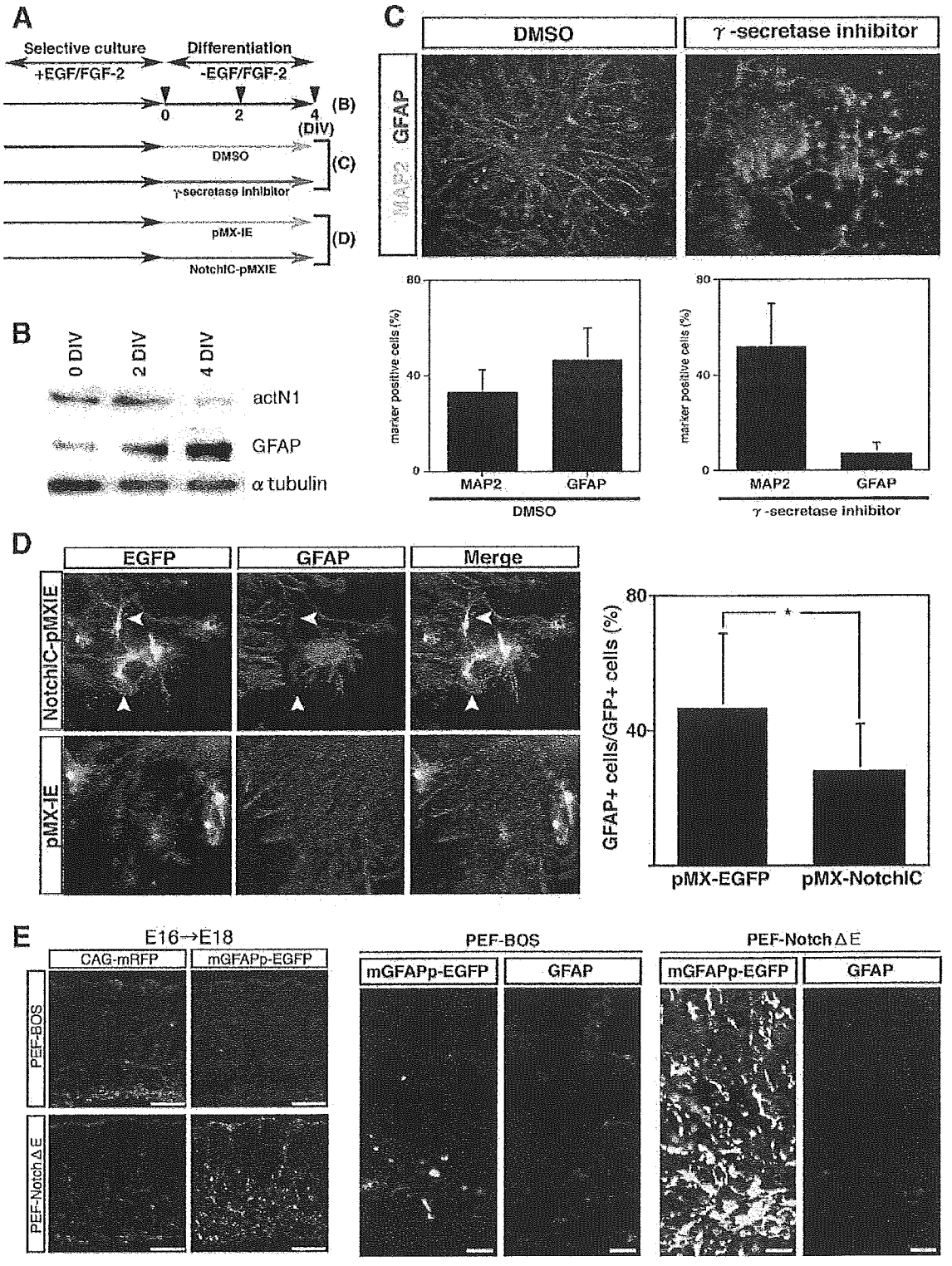

F). However, whether the effects of the persistent activation of Notch signaling, leading to a reduction in the number of GFAP-positive astrocytes, are active during the early phase of differentiation (e.g., commitment) or the later maturation phase remains uncertain.

Presently, a definitive, specific marker for committed astroglial progenitor cells that enables these cells to be distinguished from neural stem cells is not available (Kaneko et al., 2000; Tokunaga et al., 2004). However, to examine the effects of Notch activation during early astroglial differentiation, we took advantage of the fact that the transcriptional activation of GFAP starts before GFAP immunoreactivity becomes detectable in astroglial lineages (Riol et al., 1992; Morita et al., 1997). Interestingly, recent studies have suggested that the GFAP promoter contains an RBP-Jbinding sequence and may therefore be a primary target of either Notch signaling (Ge et al., 2002) and/or RBP-J/N-CoR-mediated repression (Hermanson et al., 2002). We investigated this possibility in more detail by examining the role of Notch activation in the transcriptional regulation of the GFAP gene by constructing an EGFP reporter gene under the control of a 2.5-kb mouse GFAP promoter sequence (mGFAPp) (Miura et al., 1990) (Fig. 5E). We co-transfected the mGFAPp-EGFP reporter plasmid with either pCXN2-mRFP and pEF-BOS or pEF-Notch1ΔE plasmids into E16 mouse brain and analyzed the expression of EGFP at E18. No obvious EGFP fluorescence, derived from mGFAPp, was subsequently detected in the control plasmid-electroporated brain tissue (Fig. 5E, upper left panel). On the other hand, EGFP fluorescence was enhanced by ectopically induced Notch activation (Fig. 5E, lower left panel). The transcriptional activation of mGFAP, however, was not accompanied by the expression of GFAP protein (Fig. 5E, right panel). Considering the findings of previous studies indicating that the transcriptional activation of the GFAP gene occurs in astrocytic precursors (Morita et al., 1997) prior to protein expression in mature cells, Notch signaling is likely to play an important role in either astroglial commitment or the early phase of astrocytic differentiation. Consistent with this hypothesis, we observed the ectopic expression of the immature astroglial marker glutamine synthetase (GS) (Akimoto et al., 1993; Tokunaga et al., 2004) in Notch1ΔE-expressing cells in embryonic brains (data not shown).

Discussion

Generation of a reporter system for detecting the spatial and temporal activation of Notch signaling

We report here, for the first time, a method of monitoring the activation of Notch signaling in living cells. The Venus protein is an ideal fluorescent marker in reporter analyses as it overcomes the potential limitation of a relatively slow rate of fluorescence acquisition caused by the chromophore formation of fluorescent proteins (Reid and Flynn, 1997). Furthermore, to explore the transient activation of Notch signaling, we also developed a dVenus fusion protein. Regarding the *cis*-regulatory elements, a 195-bp promoter sequence of the endogenous Notch target gene, *Hes1*, was used; this sequence contains two RBP-J binding sites. Previous reports, however, have indicated that the regulation of *Hes* genes is complicated. An in vivo study of Notch1-deficient mice suggested that *Hes1* is regulated by a pathway other than Notch signaling, since the level of *Hes1* expression was not significantly changed in *Notch1* mutant mice (de la Pompa et al., 1997). In contrast, the expression of another *Hes* family gene, *Hes5*, was reduced in Notch1 mutants, indicating that *Hes5* was responsive to Notch signaling (de la Pompa et al., 1997). Nevertheless, *Hes5* also seems to be regulated by a pathway other than Notch signaling because *Hes5* transactivation is a key step in the BMP-induced astrogliogenic switch in neural precursors (Nakashima et al., 2001). Consistent with this contention, a Smad recognition motif has been recognized to exist in the promoter region of *Hes5* (Nakashima et al., 2001).

To overcome the potential limitations of using *Hes* genes to detect RBP-J-dependent Notch activation, we utilized the minimal length promoter region, which should respond to Notch activity, and a mutant promoter to estimate RBP-J-dependent transactivation. Thus, we employed a 195-bp promoter sequence of *Hes1* and a mutant *Hes1* promoter (*Hes1*pAmBm) carrying two disrupted RBP-J sites (Fig. 1).

In regard to Notch family members, in addition to Notch1, Notch2 and Notch3 are also expressed in neural precursor cells in the ventricular/subventricular zone of developing CNS (Higuchi et al., 1995; Prakash et al., 2002). However, in contrast to Notch1 (de la Pompa et al., 1997),

Fig. 5. Notch signaling functions in astroglial commitment, but not in astroglial maturation. (A) Scheme of experiments using primary neurospheres. E14 cortical cells were cultured in the presence of EGF and bFGF (selective culture) and primary neurospheres were generated and applied for further analysis under differentiation conditions, in which the primary neurospheres were cultured in growth factor-free medium on pre-coated coverslips. (B) Immunoblotting analysis of neurospheres cultured under differentiation conditions. (C) Requirement of Notch activation in astrocyte generation. Primary neurospheres spontaneously differentiated into MAP2-positive neurons and GFAP-positive astrocytes (upper left panel). In the presence of γ-secretase inhibitors (1 μM), the proportion of GFAP-positive astrocytes decreased (upper right panel). Quantified data are shown in the lower panel ($n = 5$, respectively). (D) Effect of the persistent activation of Notch1 on astroglial differentiation. We transfect NotchIC carrying or control vector on differentiating neurospheres. The effect of transgene was analyzed by the GFAP expression in vector-carrying EGFP-positive cells. The repression of GFAP expression was observed in morphologically astrocytic cells (arrowhead). Quantification is shown in the right panel ($n = 3$, respectively, $^*P < 0.05$). (E) In vivo reporter analysis using EGFP driven by the mouse GFAP promoter. GFAP immunoreactivity did not show any difference between pEF-BOS- and pEF-Notch1ΔE-transduced brains (middle and right panel, respectively). Scale bars: 50 μm for left panel, 10 μm for middle and right panels.

the function of Notch2 and Notch3 in the CNS still remains largely unclear. In contrast to *Notch1*-deficient mice (de la Pompa et al., 1997), *Notch2*-deficient mutant mice did not exhibit disorganized somitogenesis, nor did they fail to properly regulate the expression of neurogenic genes, such as *Hes5* or *Mash1* (Hamada et al., 1999). Furthermore, the *Notch3*-deficient mice developed normally and the homozygous mutant adults were viable and fertile (Krebs et al., 2003), indicating that the *Notch3* gene is not essential for embryonic development. Notch1 therefore seems to be the major player of Notch signaling in developing CNS. Two pathways have been reported previously as a downstream of Notch signaling; RBP-J-dependent and RBP-J-independent pathways (Yamamoto et al., 2001a). The *RBP-J*-deficient mice showed severe phenotypes that resemble those of *Notch1*-deficient mice, indicating that the major Notch signaling pathway is mediated through RBP-J-dependent mechanisms (Swiatek et al., 1994; Oka et al., 1995). In the present study, we designed two reporter sets carrying RBP-J binding sequences. This series of studies provide a rationale for the reporter constructs used in the present study. However, we cannot rule out the possibility that Notch receptors other than Notch1 contributed to our reporter *trans*-activation.

Role of Notch signaling in the maintenance of neural progenitors

Notch signaling has been reported to play a role in the self-renewal capacity and maintenance of neural stem/progenitor cells (Gaiano et al., 2000; Nakamura et al., 2000; Ohtsuka et al., 2001; Hitoshi et al., 2002). To further investigate the underlying mechanisms of these processes, we confirmed that Notch signaling functions in the self-renewal of neural progenitors using an immunocytochemical analysis of neurospheres generated from E14 cortex tissue (Fig. 2A) and neurosphere-forming assays using FACS-sorted dVenus-derived fluorescence-positive neural cells (Fig. 2B). Within the neurospheres, Venus fluorescent protein expression, derived from the *Hes1*p-dVenus reporter, was selectively observed in Nestin-positive neural progenitors, but not in β-III-tubulin-positive neurons (Fig. 2A). Neurosphere-forming assays of FACS-sorted Venus-positive cells enabled the characteristics of cells in which Notch signaling had been activated at that particular time point to be determined (Fig. 2B). The neural cells with *Hes1* promoter activities also showed the highest level of neurosphere-forming activity, compared with cells expressing fluorescent signals under the control of either the EF or *Hes1*pAmBm promoter. Primary neurospheres derived from *Hes1*p-dVenus-positive cells also showed higher self-renewal and multipotent capacities, compared with neurospheres derived from *Hes1*pAmBm-dVenus-positive cells, suggesting that the RBP-J-dependent signal input is highly correlated with the maintenance of neural stem/progenitor cell states in the mouse CNS.

To the best our knowledge, this is first report documenting the live monitoring of the contribution of endogenous Notch activation to the self-renewal of neural progenitors. Our present data showing RBP-J-dependent reporter activation in the radial glia (Fig. 3 and Supplementary Fig. 4) as well as our previous report showing active Notch1 immunostaining in these cells (Tokunaga et al., 2004) lend support to the idea, because radial glia in the embryonic brain are considered to represent self-renewing neural progenitors (Malatesta et al., 2000).

Data showing the properties of cells that have been sorted according to their reporter activity and differentiation potential are shown in Fig. 2D, and the proportion of tripotent primary neurospheres generated from *Hes1*-pAmBm-Venus-expressing cells was found to decrease, suggesting the selective activation of the mutant promoter in committed progenitors. However, we cannot rule out the possibility of non-RBP-J-mediated or non-Notch signaling on our mutant reporter transactivation.

Activation of Notch signaling in gliogenesis

In the present study, we addressed the astrogliogenic function of Notch signaling by visualizing endogenous Notch activity, in a cellular context where astrogliogenesis is dominant, using several techniques, including our new reporter system, a gain-of-function analysis (Figs. 4 and 5D), and loss-of-function studies with a γ-secretase inhibitor (Fig. 5C).

Considering the results of our previous study using an antibody against activated Notch1, which showed a correlation between activated Notch1 and an astroglial progenitor marker but not the mature astrocytic marker GFAP (Tokunaga et al., 2004), we propose that Notch signaling may be selectively activated during the commitment, but not the maturation phase of astroglia differentiation. Consistent with this hypothesis, the immunoblot analysis in the present study suggested that GFAP expression was negatively correlated with the amount of the cleaved form of Notch1 (Fig. 5B). To further investigate the role of Notch signaling in astroglial development, we performed gain-of-function studies in various contexts. The ectopic expression of activated Notch1 in postnatal brain did not promote astroglial maturation (Fig. 4), but the activation of Notch signaling during the late embryonic phase promoted astroglial commitment and/or early differentiation (Fig. 5E). Consistently, neurospheres cultured with a γ-secretase inhibitor under differentiation conditions exhibited a reduction in the generation of astrocytes and a concomitant increase in the generation of neurons (Fig. 5C). As for the validity of using γ-secretase inhibitor to inhibit Notch activation, the literature is consistent in fly, zebrafish, and mice, including an in vivo demonstration (Pan et al., 2004). However, other signaling molecules have been reported to act as targets for γ-secretase inhibitor (Kopan and Ilagan, 2004). Therefore, strictly, we could not